Chapter 2
Stress Concentration Problems

Abstract Stress concentration in an elastic body may be caused mainly by the two-mechanisms i.e., concentrated forces acting to a body and geometrical discontinuities of a body such as holes or abrupt change of its surface geometry. The local stress increase induced by stress concentration sometimes causes the initiation of a fatigue crack in a structure, which must be carefully examined for engineering design. We shall first discuss the stress concentration by a concentrated applied force. Then, stress concentrations due to a circular hole and an elliptic hole are calculated by using the Airy's stress function. The general solution in a polar coordinate system derived in the previous chapter and the complex potential method discussed in Appendix A will be utilized to obtain the solutions, where the latter is essential for the analysis of elliptic hole problem, which is closely related to a crack problem to be explained in the next chapter.

Keywords Concentrated force • Elliptic hole • Stress concentration • Stress concentration factor

2.1 Mechanisms and Solution Methods of Stress Concentration

Stress concentration problems are investigated, where the stress concentration due to an external force, as well as due to structural discontinuities such as circular and elliptic holes are solved by using the Airy's stress function and the complex potentials, Timoshenko and Goodier (1970). Stress concentration in an elastic body may be caused mainly by the two mechanisms, i.e., concentrated forces acting to a body and geometrical discontinuities of a body such as holes or abrupt change of its surface geometry, Neuber (1937), Raven (1946), Peterson (1953). The local stress increase induced by stress concentration may sometimes cause the initiation of a fatigue crack in a structure, which must be carefully examined for

Y. Sumi, *Mathematical and Computational Analyses of Cracking Formation: Fracture Morphology and Its Evolution in Engineering Materials and Structures*, Mathematics for Industry 2, DOI 10.1007/978-4-431-54935-2_2, © Springer Japan 2014

engineering design. We shall first discuss the stress concentration by a concentrated applied force. Then, stress concentrations due to a circular hole and an elliptic hole are investigated. The general solution in a polar coordinate system derived in the previous chapter and the complex potential method discussed in Appendix A will be utilized to obtain the solutions, where the latter is essential for the analysis of elliptic hole problem, which is closely related to a crack problem as the length of its minor axis approaches zero.

2.2 A Concentrated Force Acting at the Tip of a Wedge

We shall consider a symmetric wedge subjected to a concentrated force at the tip, where the components of the force in the x_1- and x_2-directions are P_1 and P_2, respectively (see Fig. 2.1). The boundary conditions are expressed by

$$\sigma_\theta = \tau_{r\theta} = 0 \quad \text{on} \quad \theta = \frac{\pi}{2} \pm \alpha. \tag{2.1}$$

Using the Airy's stress function, these conditions can be rewritten as

$$\frac{\partial^2 F}{\partial r^2} = 0, \quad -\frac{\partial}{\partial r}\left(\frac{1}{r}\frac{\partial F}{\partial \theta}\right) = 0 \quad \text{on} \quad \theta = \frac{\pi}{2} \pm \alpha. \tag{2.2}$$

In order to satisfy the above conditions, $F(r, \theta)$ should be proportional to r, leading to a solution of the following form:

$$F\,(r, \theta) = c_1 r\theta \cos\theta + c_2 r\theta \sin\theta, \tag{2.3}$$

where $c_1$and c_2 are the unknown constants to be determined. Substitution of Eq. (2.3) into Eq. (1.41) leads to the stress components

$$\begin{aligned} \sigma_r &= \frac{2}{r}\left(-c_1 \sin\theta + c_2 \cos\theta\right), \\ \sigma_\theta &= \tau_{r\theta} = 0. \end{aligned} \tag{2.4}$$

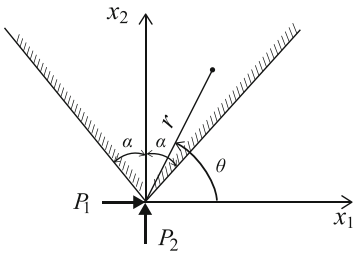

Fig. 2.1 A concentrated force acting at the tip of a wedge

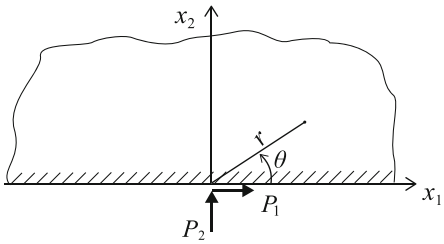

Fig. 2.2 A concentrated force acting on the surface of a semi-infinite plate

One may observe that the stress-free boundary conditions are satisfied by this expression. The equilibrium conditions for the concentrated force are represented by

$$P_1 + \int_{\pi/2-\alpha}^{\pi/2+\alpha} \sigma_r(r) \cos\theta r d\theta = 0, \tag{2.5}$$

$$P_2 + \int_{\pi/2-\alpha}^{\pi/2+\alpha} \sigma_r(r) \sin\theta r d\theta = 0, \tag{2.6}$$

with which the unknown constants are determined, and the stress distribution is obtained as

$$\sigma_r = -\frac{2}{r}\left[\frac{P_1 \cos\theta}{2\alpha - \sin 2\alpha} + \frac{P_2 \sin\theta}{2\alpha + \sin 2\alpha}\right]. \tag{2.7}$$

One may observe the stress concentration with a stress singularity of $O(r^{-1})$ near the tip of the wedge.

A concentrated force acting on the surface of a semi-infinite plate can be investigated, by simply choosing the wedge angle $\alpha = \pi/2$ (see Fig. 2.2). The corresponding solution is given by

$$\sigma_r = -\frac{2}{\pi r}(P_1 \cos\theta + P_2 \sin\theta), \quad \sigma_\theta = \tau_{r\theta} = 0. \tag{2.8}$$

The stress components in the linear orthogonal coordinate system $O - x_1x_2$ are calculated as

$$\sigma_{11} = -\frac{2P_1}{\pi x_1}, \quad \sigma_{22} = \sigma_{12} = 0, \tag{2.9}$$

on the plate surface, so that the stress distribution exhibits a stress singularity as illustrated in Fig. 2.3.

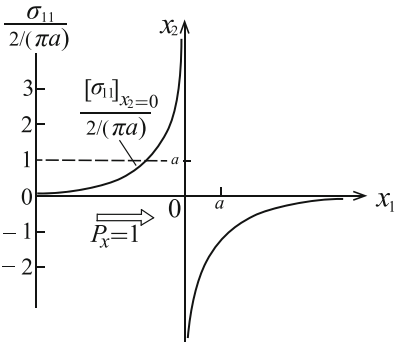

Fig. 2.3 Stress singularity on the surface near the concentrated force

2.3 Axisymmetric Solution

The axisymmetric parts of the solution of a two-dimensional problem can be derived from Eq. (1.68), and obtained as

$$F(r) = r^2 (a_0 + b_0 \ln r) + a_0' + b_0' \ln r. \tag{2.10}$$

The corresponding stress distribution is calculated as

$$\begin{aligned} \sigma_r &= \frac{1}{r}\frac{dF}{dr} = 2a_0 + b_0 (2\ln r + 1) + \frac{b_0'}{r^2} \\ \sigma_\theta &= \frac{d^2F}{dr^2} = 2a_0 + b_0 (2\ln r + 3) - \frac{b_0'}{r^2} \\ \tau_{r\theta} &= 0. \end{aligned} \tag{2.11}$$

The displacement field is represented by the radial component u_r, and the corresponding strain components are calculated as

$$\varepsilon_r = \frac{du_r}{dr},\ \varepsilon_\theta = \frac{u_r}{r},\ \gamma_{r\theta} = 0, \tag{2.12}$$

where an additional compatibility condition

$$\varepsilon_r = \varepsilon_\theta + r\frac{d\varepsilon_\theta}{dr}, \tag{2.13}$$

should hold. Using the stress–strain relation in plane stress condition, the compatibility condition is expressed in terms of stress

$$(1+\nu)(\sigma_r - \sigma_\theta) = r\left(\frac{d\sigma_\theta}{dr} - \nu\frac{d\sigma_r}{dr}\right). \tag{2.14}$$

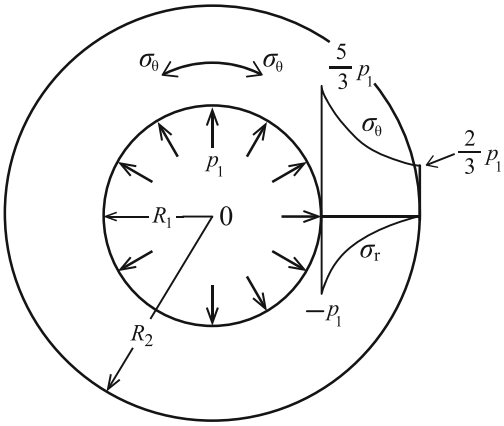

Fig. 2.4 Thick cylinder subjected to internal pressure

Substituting Eq. (2.11) into Eq. (2.14), one can obtain

$$b_0 = 0, \tag{2.15}$$

so that the stress distribution is given by

$$\sigma_r = 2a_0 + \frac{b_0'}{r^2},\ \sigma_\theta = 2a_0 - \frac{b_0'}{r^2},\ \tau_{r\theta} = 0. \tag{2.16}$$

If the origin exists inside the body, the singular term of $O(r^{-2})$ vanishes and a constant stress distribution is attained.

Suppose a thick cylinder with its inner radius, R_1 and outer radius, R_2 subjected to internal pressure p_1 and external pressure p_2, respectively. Having substituted Eq. (2.16) into the boundary conditions,

$$\sigma_r\,(r = R_1) = -p_1,\ \sigma_r\,(r = R_2) = -p_2, \tag{2.17}$$

the stress distribution is obtained as

$$\begin{aligned}
\sigma_r &= -\frac{(p_1 - p_2)\,R_1^2 R_2^2}{R_2^2 - R_1^2}\frac{1}{r^2} + \frac{p_1 R_1^2 - p_2 R_2^2}{R_2^2 - R_1^2},\\
\sigma_\theta &= \frac{(p_1 - p_2)\,R_1^2 R_2^2}{R_2^2 - R_1^2}\frac{1}{r^2} + \frac{p_1 R_1^2 - p_2 R_2^2}{R_2^2 - R_1^2},\\
\tau_{r\theta} &= 0,
\end{aligned} \tag{2.18}$$

where one can observe the stress concentration of the circumferential (hoop) stress near the internal surface of the cylinder. Figure 2.4 shows the results of stress distribution for the cylinder ($R_2/R_1 = 2$) subjected to only the internal pressure p_1, in which one can clearly see the stress concentration on the internal surface of

the cylinder. In case of $R_1 = 0$, we have a solid cylinder with a hydrostatic stress equal to the external pressure. A circular hole in an infinite medium is obtained as the limit of $R_2 \to \infty$, and the solution becomes

$$\begin{aligned} \sigma_r &= -p_1 \left(R_1/r\right)^2 \\ \sigma_\theta &= p_1 \left(R_1/r\right)^2 . \end{aligned} \tag{2.19}$$

If we superimpose a biaxial uniform stress $\sigma_0 = p_1$, to the above solution, the stress-free condition is attained on the circular hole and the solution becomes

$$\begin{aligned} \sigma_r &= \sigma_0 \left\{1 - \left(R_1/r\right)^2\right\} \\ \sigma_\theta &= \sigma_0 \left\{1 + \left(R_1/r\right)^2\right\}. \end{aligned} \tag{2.20}$$

The hoop stress is maximized on the hole surface with its magnitude twice as high as the biaxial remote stress.

2.4 Stress Concentration Caused by a Circular Hole

In this section, we shall consider the stress distribution near a circular hole of diameter, R, in an infinite plate subjected to uniaxial tensile stress, σ_0, as illustrated in Fig. 2.5. The boundary conditions far away from the hole are given by

$$\left.\begin{aligned} \sigma_{11} &= \sigma_0 \\ \sigma_{22} = \sigma_{12} &= 0 \end{aligned}\right\} \text{ at } |x_1| \longrightarrow \infty, \tag{2.21}$$

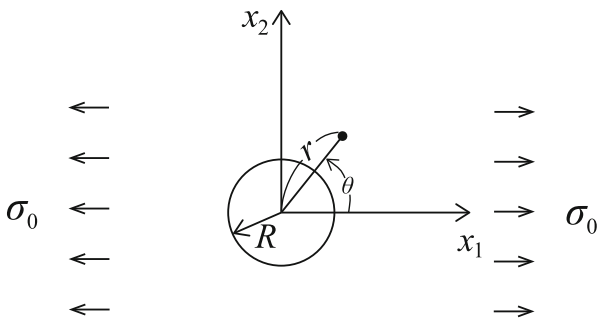

Fig. 2.5 Stress distribution near a circular hole

and the corresponding stress function, F_0, is

$$F_0 = \frac{1}{2}\sigma_0 x_2^2, \tag{2.22}$$

while the boundary conditions on the circular hole are

$$\sigma_r = \tau_{r\theta} = 0. \tag{2.23}$$

The stress function, F, can be expressed by

$$F = F_0 + F_1 = \frac{1}{4}\sigma_0 r^2 (1 - \cos 2\theta) + F_1 (r, \theta), \tag{2.24}$$

by adding the correctional term, F_1, due to the hole, and the stress components on the hole are given by

$$\left.\begin{aligned} \sigma_r &= \frac{1}{2}\sigma_0 (1 + \cos 2\theta) + \frac{1}{r^2}\frac{\partial^2 F_1}{\partial \theta^2} + \frac{1}{r}\frac{\partial F_1}{\partial r} = 0 \\ \tau_{r\theta} &= \frac{1}{2}\sigma_0 \sin 2\theta - \frac{\partial}{\partial r}\left(\frac{1}{r}\frac{\partial F_1}{\partial \theta}\right) = 0 \end{aligned}\right\} \text{ on } r = R. \tag{2.25}$$

Therefore, the stress function, F_1, should be composed of the axisymmetric part and the term proportional to $\cos 2\theta$ in Eq. (1.68), whose stress components diminish at infinity. The result is

$$F_1 (r, \theta) = b_0' \ln r + b_2 \cos 2\theta + b_2' r^{-2} \cos 2\theta. \tag{2.26}$$

From Eq. (2.25), one can determine the unknown coefficients b_0', b_2, and b_2', and the stress distribution is obtained as

$$\begin{aligned} \sigma_r &= \frac{\sigma_0}{2}\left[\left\{1 - (R/r)^2\right\} + \left\{1 - 4(R/r)^2 + 3(R/r)^4\right\}\cos 2\theta\right], \\ \sigma_\theta &= \frac{\sigma_0}{2}\left[\left\{1 + (R/r)^2\right\} - \left\{1 + 3(R/r)^4\right\}\cos 2\theta\right], \\ \tau_{r\theta} &= -\frac{\sigma_0}{2}\left\{1 + 2(R/r)^2 - 3(R/r)^4\right\}\sin 2\theta. \end{aligned} \tag{2.27}$$

Figure 2.6 illustrates the stress distribution near the hole, in which the maximum stress $\sigma_{11} = 3\sigma_0$ is attained at the edge of the hole.

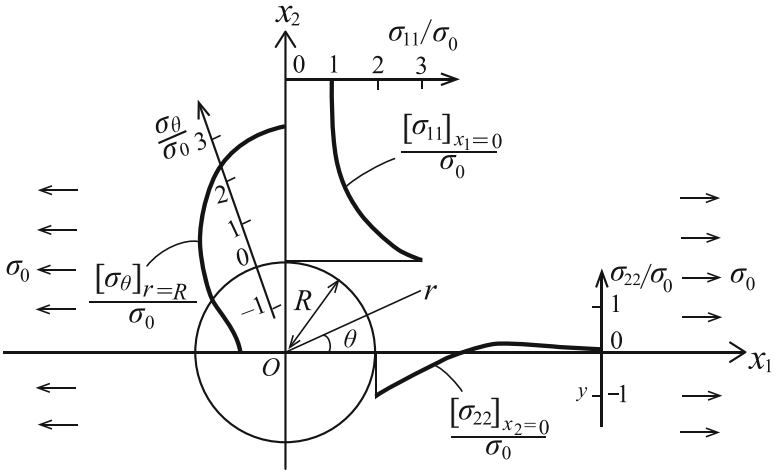

Fig. 2.6 Stress distribution near a circular hole

2.5 Stress Concentration Factor

In order to quantify the magnitude of stress concentration, a stress concentration factor, α, is often employed in engineering design, which is defined by

$$\alpha \equiv (\text{local maximum stress}) / (\text{nominal stress}). \tag{2.28}$$

In the case of a circular hole in uniaxial tension, the stress concentration factor $\alpha = 3$, while the same hole in biaxial tension as illustrated in Fig. 2.7a exhibits less stress concentration, $\alpha = 2$. In the case of pure shear loading, it may be decomposed to the biaxial tension and compression of the same magnitude, so that the stress concentration is higher, i.e., $\alpha = 4$ (see Fig. 2.7b).

As will be discussed in detail in the next section, the stress concentration factor of an elliptic hole in uniaxial tension is expressed by

$$\alpha = 1 + 2\,(a/b), \tag{2.29}$$

where the lengths of the major and minor axes of the ellipse are denoted by a and b, respectively (Inglis 1913). The lengths of major and minor axes, and the radius of curvature at the root of the hole are related by

$$\rho = b^2/a, \tag{2.30}$$

so that one can rewrite Eq. (2.29) into

$$\alpha = 1 + 2\sqrt{a/\rho}. \tag{2.31}$$

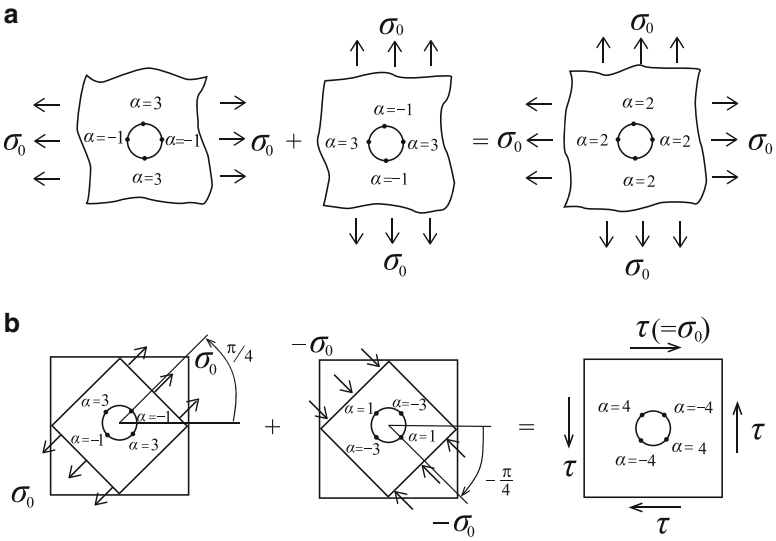

Fig. 2.7 Stress concentration under (**a**) biaxial tension and (**b**) pure shear

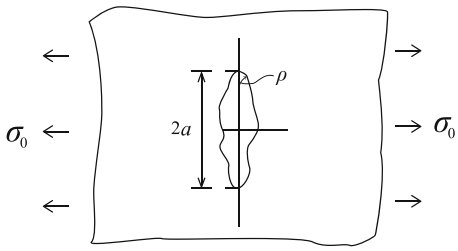

Fig. 2.8 Stress concentration due to a defect under uniaxial tension

This expression is known to be applicable to the estimation of the stress concentration factor of a wider range of internal defects whose projected length on the plane perpendicular to the principal loading direction is $2a$ and its tip radius is ρ (see Fig. 2.8).

2.6 Elliptic Hole in Tension

We shall consider an elliptic hole in tension as illustrated in Fig. 2.9, where the major and minor axes of the ellipse are a and b, respectively, and the major axis is at angle β to the loading direction, Inglis (1913), Stevenson (1945). We shall introduce the two linear Cartesian coordinate systems, i.e., the $O-x_1x_2$ coordinate system, whose directions coincide with the major and minor axes of the ellipse, and the $O-x_1'x_2'$

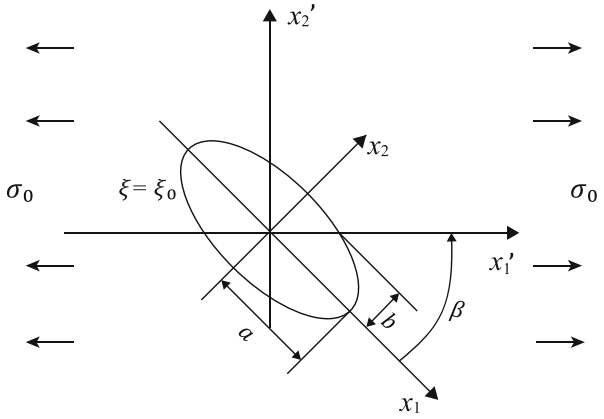

Fig. 2.9 An inclined elliptic hole under uniaxial tension

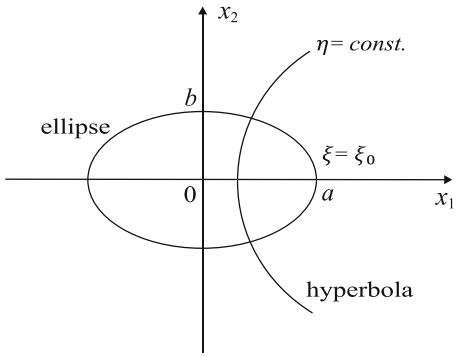

Fig. 2.10 Elliptic coordinate system

coordinate system being at angle β to the $O - x_1x_2$ coordinate system. The elliptic coordinate system (ξ, η) illustrated in Fig. 2.10 can be defined by

$$z = f(\varsigma) = c\cosh\varsigma, \quad \zeta = \xi + i\eta. \tag{2.32}$$

Its real and imaginary parts are calculated as

$$x_1 = c\cosh\xi\cos\eta \text{ and } x_2 = c\sinh\xi\sin\eta, \tag{2.33}$$

and its derivative is

$$\frac{dz}{d\zeta} = c\sinh\zeta \equiv Je^{i\alpha}, \tag{2.34}$$

where

$$J^2 = \frac{1}{2}c^2(\cosh 2\xi - \cos 2\eta), \tag{2.35}$$

and

$$e^{2i\alpha} = \frac{\sinh\zeta}{\sinh\bar{\zeta}}\,,\quad \tan\alpha = \coth\xi\tan\eta. \tag{2.36}$$

Assuming that the elliptic hole corresponds to $\xi = \xi_0$, we have

$$a = c\cosh\xi_0\,,\, b = c\sinh\xi_0, \tag{2.37}$$

so that

$$c = a\sqrt{1-(b/a)^2}\,,\, \xi_0 = \operatorname{arctanh}(b/a). \tag{2.38}$$

In order to avoid the multiple-valueness of the displacement and stresses, periodic analytic functions such as $\sinh n\zeta$ and $\cosh n\zeta$ may be selected as the possible candidates of the solution.

The stress components in terms of the $O - x_1'x_2'$ coordinate system are transformed from those in terms of the $O - x_1x_2$ coordinate system by Eq. (A.47) (see Appendix A). Therefore, the boundary conditions at infinity can be expressed by

$$\left.\begin{aligned}&\sigma_{11}+\sigma_{22} = \sigma_0\\ &\sigma_{22}-\sigma_{11}+2i\sigma_{12} = -\sigma_0 e^{-2i\beta}\end{aligned}\right\}\ \text{at infinity}, \tag{2.39}$$

while those on the elliptic hole are given by

$$\sigma_\xi - i\,\tau_{\xi\eta} = \psi'(z) + \overline{\psi'(z)} - e^{2i\alpha}\left[\bar{z}\psi''(z) + \chi'(z)\right] = 0. \tag{2.40}$$

Stevenson (1945) derived the complex potentials of the solution in the following form:

$$\begin{aligned}4\psi(z) &= Ac\cosh\zeta + Bc\sinh\zeta,\\ 4\chi(z) &= Cc^2\zeta + Dc^2\cosh 2\zeta + Ec^2\sinh 2\zeta,\end{aligned} \tag{2.41}$$

in which A and C are real, while B, D, and E are complex unknown constants, respectively, given by

$$B = B_1 + iB_2,\quad D = D_1 + iD_2,\quad E = E_1 + iE_2. \tag{2.42}$$

Substituting Eq. (2.42) into Eq. (2.41), the boundary condition at infinity (Eq. (2.39)) leads to

$$\begin{aligned}A + B_1 &= \sigma_0,\\ 2(D+E) &= -\sigma_0 e^{-2i\beta}.\end{aligned} \tag{2.43}$$

The boundary conditions on the elliptic hole is calculated by Eq. (2.40) with Eq. (2.41) where the stress-free condition on the hole edge $\xi = \xi_0$, is given by

$$\begin{aligned} 4\left(\sigma_\xi - i\tau_{\xi\eta}\right) = \operatorname{cosech}\overline{\zeta}\Big[& (2A + B)\coth\zeta\sinh\overline{\zeta} \\ & + \left(\overline{B} + B\operatorname{cosech}^2\zeta\right)\cosh\overline{\zeta} + (C + 2E)\operatorname{cosech}\zeta\coth\zeta \\ & -4D\sinh\zeta - 4E\cosh\zeta\Big] = 0. \end{aligned} \tag{2.44}$$

This condition can be rewritten as

$$\begin{aligned} & (2A\sinh 2\xi_0 - 2iB_2\cosh 2\xi_0 - 4E)\cosh\zeta \\ & -(2A\cosh 2\xi_0 - 2iB_2\sinh 2\xi_0 + 4D)\sinh\zeta \\ & +(C + 2E + B\cosh 2\xi_0)\coth\zeta\operatorname{cosech}\zeta = 0. \end{aligned} \tag{2.45}$$

The five unknown constants are determined by the five independent conditions represented by Eqs. (2.43) and (2.45), so that the complete form of the complex potentials has been obtained as

$$\begin{aligned} 4\psi(z) &= c\sigma_0\left[e^{2\xi_0}\cos 2\beta\cosh\zeta + \left(1 - e^{2\xi_0 + 2i\beta}\right)\sinh\zeta\right], \\ 4\chi(z) &= -c^2\sigma_0\left[(\cosh 2\xi_0 - \cos 2\beta)\,\zeta + \frac{1}{2}e^{2\xi_0}\cosh 2\left(\zeta - \xi_0 - i\beta\right)\right]. \end{aligned} \tag{2.46}$$

The normal stress along the hole edge is calculated by Eq. (A.46)

$$\sigma_\eta(\xi = \xi_0) = \sigma_0\frac{\sinh 2\xi_0 + \cos 2\beta - e^{2\xi_0}\cos 2(\beta - \eta)}{\cosh 2\xi_0 - \cos 2\eta}. \tag{2.47}$$

In the case where the major axis is perpendicular to the loading direction, $\beta = \pi/2$, the above result is simplified as

$$\sigma_\eta(\xi = \xi_0) = \sigma_0 e^{2\xi_0}\left[\frac{\sinh 2\xi_0\left(1 + e^{-2\xi_0}\right)}{\cosh 2\xi_0 - \cos 2\eta} - 1\right], \tag{2.48}$$

and the maximum stress is attained at $\eta = 0$ and π by

$$\left(\sigma_\eta\right)_{\max} = \sigma_0\left\{1 + 2(a/b)\right\}, \tag{2.49}$$

as observed in Eq. (2.29). Similar to the consideration of the superposition of biaxial tension and compression in Fig. 2.7b, the solution of the loading condition under pure shear, τ, is obtained by adding the two solutions of $\sigma_0 = \tau$ with $\beta = \pi/4$, and

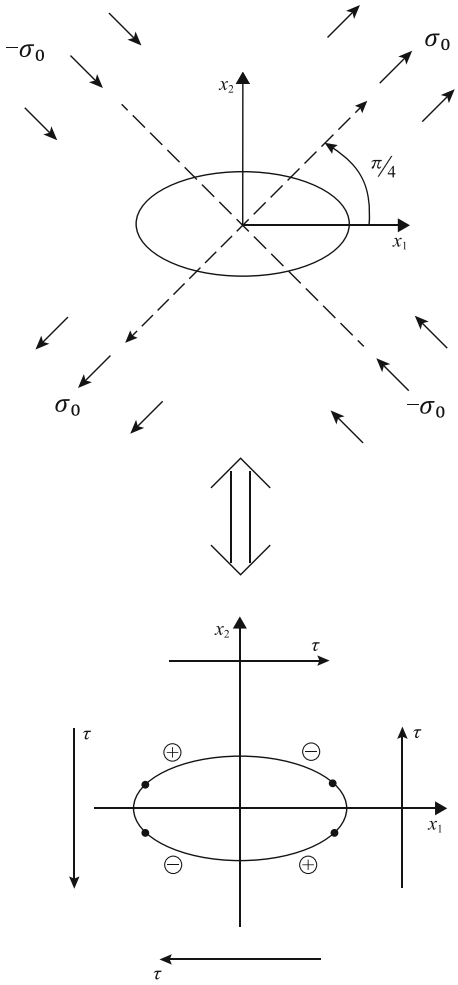

Fig. 2.11 Elliptic hole under pure shear

$\sigma_0 = -\tau$ with $\beta = 3\pi/4$ for Eq. (2.46), and the normal stress acting along the hole edge is calculated as

$$\sigma_\eta\left(\xi = \xi_0\right) = -2\tau \frac{e^{2\xi_0} \sin 2\eta}{\cosh 2\xi_0 - \cos 2\eta}. \tag{2.50}$$

The maximum stress is attained at the points shown in Fig. 2.11, where the condition

$$\cos\eta = 1/\sqrt{1 + (b/a)^2}, \tag{2.51}$$

is satisfied, and its value is calculated as

$$\sigma_\eta\left(\xi = \xi_0, \cos\eta = 1/\sqrt{1 + (b/a)^2}\right) = \pm\tau \frac{(a+b)^2}{ab}. \tag{2.52}$$

References

Inglis CE (1913) Stresses in a plate due to the presence of cracks and sharp corners. Trans Roy Inst Naval Architects 55-1:219–241

Neuber H (1937) Kerbspannungslehre: grundlagen fur genaue spannugsrechnung. Springer, Berlin

Peterson RE (1953) Stress concentration design factors. Wiley, New York

Raven FA (1946) Theory of notch stresses: principle of exact stress calculation, (translation of Neuber, 1937). U.S. Navy Department, David Taylor Model Basin, Washington, D.C.

Stevenson AC (1945) Complex potentials in two-dimensional elasticity. Proc Roy Soc Lond A 184:129–179

Timoshenko SP, Goodier JN (1970) Theory of elasticity, 3rd edn. McGraw-Hill, New York

http://www.springer.com/978-4-431-54934-5

Mathematical and Computational Analyses of Cracking Formation
Fracture Morphology and Its Evolution in Engineering Materials and Structures
Sumi, Y.
2014, XII, 282 p. 168 illus., 12 illus. in color., Hardcover
ISBN: 978-4-431-54934-5